A Comparison of Solution, Microcrystalline Solid, and Thin Film Phase Voltammetry of $[Co(mtas)_2](X)_n$ (mtas = Bis(2-(dimethylarsino)phenyl)methylarsine; X = BF_4^-, n = 3; X = ClO_4^-, n = 2, 3; X = BPh_4^-, n = 2)

Alison J. Downard,*,† Alan M. Bond,*,‡ Lyall R. Hanton,§ and Graham A. Heath‖

School of Chemistry, La Trobe University, Bundoora, Victoria 3083, Australia, Department of Chemistry, University of Otago, Dunedin, New Zealand, and Research School of Chemistry, Australian National University, Canberra, ACT, Australia

Received November 22, 1994⊗

The voltammetry of water insoluble microcrystalline forms of $[Co(mtas)_2](ClO_4)_3$, $[Co(mtas)_2](ClO_4)_2$ and $[Co(mtas)_2](BPh_4)_2$ (mtas = bis(2-(dimethylarsino)phenyl)methylarsine), mechanically attached to basal plane graphite electrodes has been studied in aqueous perchlorate electrolytes. For $[Co(mtas)_2](ClO_4)_3$ and $[Co(mtas)_2](ClO_4)_2$ the Co(III)/Co(II) and Co(II)/Co(I) processes are consistent with a model of electron transfer within a thin layer of electroactive material on or near to the surface of microcrystalline particles, with the bulk of the solid undergoing diffusion-controlled reactions at relatively slow rates. Interestingly, oxidation of BPh_4^- is necessary before a pronounced voltammetric response occurs for $[Co(mtas)_2](BPh_4)_2$. Experimental data suggest that ion-pairing effects and the hydrophobicity of the solid control the electrochemical behavior in the solid-state studies. The visible spectra of Co(III) and Co(II) complexes in solution and in the solid state are consistent with similar electronic and molecular structures for each oxidation state in both phases. However, the potential of the Co(III)/Co(II) couple obtained with $[Co(mtas)_2](BF_4)_3$ dissolved in aqueous medium is approximately 170 mV more negative than for the same couple in the microcrystalline solids. The Co(II)/Co(I) couple occurs at a similar potential in both solid and solution phases. Voltammetry in the aqueous solution phase at a glassy carbon electrode results in the deposition of a self-limiting, continuous film of electrochemically insulating $[Co(mtas)_2]Cl$ or $[Co(mtas)_2](BF_4)$ and highlights the importance of the microcrystalline morphology for the observation of well-defined voltammetry of nonconducting solid materials.

Introduction

The redox properties of inorganic complexes are most often examined by voltammetry of aqueous or non-aqueous solutions of the complexes.[1,2] Also well-established is the study of electroactive species incorporated into insoluble polymers on electrode surfaces or attached as a monolayer to the electrode surface via covalent bonds or by chemisorption.[3,4] Recently it has been demonstrated that it is also possible to observe well-defined electrochemistry arising from nonconducting solids in the form of microcrystalline particles mechanically attached to carbon electrodes.[5−8] It appears that rapid charge-transport may occur via the large three-phase boundary (electrode/solid/solution) that exists at sufficiently small particles, giving rise to easily measurable currents. In this manner the voltammetry of water-insoluble decamethylferrocene[5], *cis*- and *trans*-$Cr(CO)_2(dpe)_2$ and *trans*-$[Cr(CO)_2(dpe)_2]^+$ (dpe = $Ph_2PCH_2CH_2PPh_2$),[6,7] and salts of the Dawson anion $[S_2Mo_{18}O_{62}]^{4-}$ [8] has been examined in aqueous solutions. For the former complexes, two different types of electrochemical behavior were observed. The chromium complexes exhibited predominantly "thick layer" (diffusion-controlled) voltammetry, and incorporation of ClO_4^-, accompanying oxidation of *cis*- $Cr(CO)_2(dpe)_2$, was readily observed by X-ray electron probe analysis when the aqueous solution contained $KClO_4$ as the electrolyte. The voltammetric response of decamethylferrocene was consistent with predominantly "thin layer" electrochemistry and large peak-to-peak separations (ΔE_p values) were attributed to solid state changes concurrent with electron transfer. X-ray electron probe analysis demonstrated uptake of ClO_4^- on oxidation, and complete electrolysis of the attached solid was assumed to occur during cyclic voltammetry at a slow scan rate (10 mV s^{-1}). The initial studies demonstrate that electrochemical measurements on nonconducting solids in microcrystalline form are surprisingly accessible. However, the factors that determine the response remain unclear as does the relationship between solution and solid phase voltammetry in the same medium. To expand this new area of electrochemistry we wished to extend studies on the solid phase voltammetry of highly charged complexes. For an appropriately charged complex, judicious choice of the counterion should make it possible to synthesize both water soluble and water insoluble forms. Thermodynamic comparisons of the microcrystalline and dissolved solid in aqueous media are then possible, enabling the effect of the solid environment on redox potentials to be assessed. Additionally, a study of charged complexes enables the influence of the

† La Trobe University. On leave from the University of Canterbury, Christchurch, New Zealand.

‡ La Trobe University. Present Address for correspondence: Department of Chemistry, Monash University, Clayton, Victoria, 3168, Australia.

§ University of Otago.

‖ Australian National University.

⊗ Abstract published in *Advance ACS Abstracts,* October 1, 1995.

(1) Bard, A. J., Ed. *Encyclopedia of Electrochemistry of the Elements*; Marcel Dekker: New York, 1973−1976; Vols. I−X.
(2) Pombeiro, A. J. K., McCleverty, J. A., Eds. *Molecular Electrochemistry of Inorganic, Bioinorganic and Organometallic Compounds*; NATO ASI, Series C: Mathematical and Physical Sciences; Kluwer: Dordrecht, The Netherlands 1993; Vol. 385.
(3) Murray, R. W. *Acc. Chem. Res.* **1980**, *13*, 135.
(4) Abruña, H. D. *Coord. Chem. Rev.* **1988**, *86*, 135.
(5) Bond, A. M.; Marken, F. *J. Electroanal. Chem.* **1994**, *372*, 125.
(6) Bond, A. M.; Colton, R.; Daniels, F.; Fernando, D. R.; Marken, F.; Nagaosa, Y.; Van Stevenick, R. F. M.; Walter, J. N. *J. Am. Chem. Soc.* **1993**, *115*, 9556.
(7) Bond, A. M.; Colton, R.; Marken, F.; Walter, J. N. *Organometallics* **1994**, *13*, 5122.
(8) Bond, A. M.; Cooper, J. B.; Marken, F.; Way, D. M.; Wedd, A. G. *J. Electroanal. Chem.*, in press.

0020-1669/95/1334-6387$09.00/0

Table 1. Voltammetric Data (Scan Rate = 100 mV s^{-1}) for Cobalt Complexes[a]

$[Co(mtas)_2]X_n$					$E_{1/2}$/V[c]		
X	*n*	phase	electrolyte (0.1 M)	electrode[b]	Co(III)/Co(II)	Co(II)/Co(I)	Co(I)/Co(0)
BF_4^-	3	solution	CH_3CN/Bu_4NClO_4	gc	0.04(60)	−0.61(60)	−1.85(66)
BPh_4^-	2	solution	CH_3CN/Bu_4NPF_6	gc	0.04(62)	−0.61(62)	−1.86(74)
BPh_4^-	2	solution	CH_2Cl_2/Bu_4NPF_6	gc	0.14(86)	−0.57(78)	−2.05[d]
ClO_4^-	3	solid	$H_2O/LiClO_4$	bpg	0.05(54)	−0.61(90)	
ClO_4^-	2	solid	$H_2O/LiClO_4$	bpg	0.04(50)	−0.61(60)	
BPh_4^-	2	solid	$H_2O/LiClO_4$	bpg	0.03(36)	−0.63(60)	
BF_4^-	3	solution	H_2O/LiCl	bpg	−0.13(60) −0.06(40)[e]		
BF_4^-	3	solution	H_2O/LiCl	gc	−0.13(72)	−0.60(120)[e]	

[a] 1 mM complex for solution studies. [b] Key: gc = glassy carbon; bpg = basal plane graphite. [c] $E_{1/2} = (E_p^{ox} + E_p^{red})/2$; Corrected to V vs SCE (nonaqueous solvents), V vs Ag/AgCl (3 M NaCl) (aqueous electrolytes); values in parentheses indicate ΔE_p values in mV. [d] E_p^{red} for irreversible reduction. [e] Adsorption controlled response.

counterion on the electrochemistry to be examined. Unlike the case with redox studies on dissolved species, it is feasible that the counterion incorporated in the solid might exert a significant effect on the electrochemical response of the complex.

The present study concerns the complexes $[Co(mtas)_2](BF_4)_3$,[9] $[Co(mtas)_2](ClO_4)_3$, $[Co(mtas)_2](ClO_4)_2$,[10] and $[Co(mtas)_2](BPh_4)_2$ (mtas = bis(2-(dimethylarsino)phenyl)methylarsine, see structure **1**). This choice was based on the ease of preparing

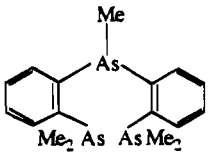

1

water soluble and insoluble salts of $[Co(mtas)_2]^{3+}$ and the availability of stable Co(III) and Co(II) forms of the complexes. Furthermore, the voltammetric response of both forms is known to be well-defined in organic solvents.[11,12] We describe the voltammetry in aqueous electrolyte of dissolved $[Co(mtas)_2](BF_4)_3$ and of microcrystalline forms of $[Co(mtas)_2](ClO_4)_3$, $[Co(mtas)_2](ClO_4)_2$ and $[Co(mtas)_2](BPh_4)_2$ mechanically attached to pyrolytic basal plane graphite electrodes. We were also able to establish conditions which led to the electrodeposition of films of the divalent complex on the electrode surface, and hence for the first time we are able to compare the $[Co(mtas)]^{3+/2+}$ and $[Co(mtas)2]^{2+/+}$ responses for the dissolved species, the mechanically attached microcrystalline solid, and the electrodeposited film, all in aqueous electrolytes.

Experimental Section

Chemicals. All reagents were of analytical or electrochemical grade purity, and Millipore water having a resistivity of 17.2 MΩ cm^{-1} was used for the preparation of aqueous electrolytes. The complex $[Co(mtas)_2](BF_4)_3$ was synthesized following a literature procedure.[9] $[Co(mtas)_2](ClO_4)_3$ and $[Co(mtas)_2](BPh_4)_2$ were prepared by dissolving $[Co(mtas)_2](BF_4)_3$ in a minimum of water and adding an aqueous solution of $NaClO_4$ or $NaBPh_4$ until precipitation occurred. In each case the product was collected by filtration. On addition of $NaBPh_4$(aq) to the solution of $[Co(mtas)_2](BF_4)_3$ the solution changed color from yellow-orange to yellow-green, and the product was subsequently identified as $[Co(mtas)_2](BPh_4)_2$. $[Co(mtas)_2](ClO_4)_2$ was prepared by dissolving a small sample of $[Co(mtas)_2](ClO_4)_3$ in a minimum of acetone and diluting 5-fold with water. A nitrogen atmosphere was maintained over the solution and an aqueous solution of $NaBH_4$ was added dropwise until precipitation occurred. The yellow-green product was collected by filtration and air-dried. For all complexes, the oxidation state was confirmed using steady-state voltammetry of the sample dissolved in acetonitrile containing 0.1 M Bu_4NPF_6 at a 10 μm diameter platinum disk microelectrode and noting the sign of the current for the Co(III)/Co(II) process. Clearly at the reversible Co(III)/Co(II) potential Co(III) compounds are reduced and Co(II) compounds are oxidized and this feature provides a ready distinction between the two oxidation states. The long term stabilities of the Co(II) and Co(III) complexes as the solids were also monitored in the same way and all solids were found to be stable as isolated for the duration of the study.

Electrochemical Instrumentation and Methods. Cyclic voltammetric measurements were made using either a Cypress Systems Model CS-1090 Computer-Controlled Electroanalytical System, a BAS 100 electrochemical analyzer, or a PAR Model 174A polarographic analyzer coupled to a PAR Model 175 universal programmer. Working electrodes used for solution measurements were glassy carbon or basal plane pyrolytic graphite disks (area = 0.07 and 0.13 cm^2, respectively) mounted in Teflon or a platinum or glassy carbon disk microelectrode (10 μm and 11 μm diameter, respectively) sealed in glass. Experiments involving mechanically attached solids utilized a basal plane pyrolytic graphite disk (area = 0.17 cm^2) mounted in Teflon. The auxiliary electrode was a platinum wire. For measurements in aqueous solution, the reference electrode was Ag/AgCl (3 M NaCl) and in acetonitrile and dichloromethane, a Ag/Ag^+ (0.01 M in CH_3CN/0.1 M Bu_4NPF_6) reference electrode was used. Potentials in the organic solvents are reported *vs* SCE after referencing to *in situ* ferrocene ($E^{o\prime}$ = 0.31 V vs SCE).[13] Unless stated otherwise, all solutions were degassed with nitrogen prior to measurement and data were obtained at (20 ± 2) °C. Attachment of microcrystalline solids to the graphite electrode was achieved by placing a small sample of the solid on a filter paper and rubbing the surface of the basal plane graphite over the solid. The electrode surface was renewed by dissolving the solid with acetone or cleaving a thin layer of graphite from the surface with a razor blade.

Diffuse Reflectance Spectroscopy and Spectroelectrochemistry. Diffuse reflectance spectra of solid samples were obtained employing a CARY 5 Scanning Spectrometer with a Harrick Preying Mantis reflectance accessory. The samples were diluted 10-fold with $NaBF_4$ and finely ground. For spectroelectrochemical experiments, electronic absorption spectra were recorded using a Perkin-Elmer Lambda 9 double-beam spectrometer. The absorbing species were generated in an optically transparent electrochemical cell mounted in the spectrometer. The three-compartment cell comprised a Pt gauze working electrode positioned in the optical beam, a Pt wire auxiliary and Ag/AgCl reference electrode (both outside the beam). The path length of the cell was 0.5 mm and the required species was generated by applying an over-potential of approximately 150 mV. The cell was cooled by a stream of cold, dry, nitrogen gas and the temperature was controlled using a Bruker B-VT 1000 control unit and heater element.

(9) Fitzpatrick, M. G.; Hanton, L. R.; Levason, W.; Spicer, M. D. *Inorg. Chim. Acta* **1988**, *142*, 17.
(10) Cunninghame, R. G.; Nyholm, R. S.; Tobe, M. L. *J. Chem. Soc.* **1964**, 5800.
(11) Downard, A. J.; Hanton, L. R.; Paul, R. L. *J. Chem. Soc., Chem Commun.* **1992**, 235.
(12) Downard, A. J.; Hanton, L. R.; McMoran, D. A.; Paul, R. L. *Inorg. Chem.* **1993**, *32*, 6028.
(13) Bard, A. J.; Faulkner, L. R. *Electrochemical Methods*; Wiley: New York, 1980; p 701.

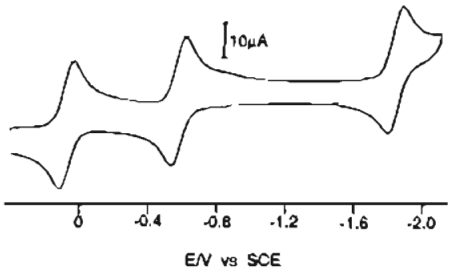

Figure 1. Cyclic voltammogram of [Co(mtas)$_2$](BF$_4$)$_3$ (1 mM) recorded in acetonitrile containing 0.1 M Bu$_4$NClO$_4$ at a glassy carbon electrode. Scan rate = 100 mV s^{-1}.

Electron Probe X-ray Microanalysis. The instrument and sample preparation procedures used for electron-probe X-ray measurements have been described previously.[5,6,8]

Results

Solution-Phase Voltammetry and Spectroelectrochemistry in Acetonitrile and Dichloromethane. Figure 1 shows a cyclic voltammogram of 1 mM [Co^{III}(mtas)$_2$](BF$_4$)$_3$ in acetonitrile containing 0.1 M Bu$_4$NClO$_4$ recorded at a scan rate of 100 mV s^{-1} at a glassy carbon electrode. Three essentially reversible one-electron reduction steps are observed which may be represented by eqs 1−3. The voltammetry of [Co^{III}(mtas)$_2$]-

$$[Co(mtas)_2]^{3+} + e^- \rightleftharpoons [Co(mtas)_2]^{2+} \quad (1)$$

$$[Co(mtas)_2]^{2+} + e^- \rightleftharpoons [Co(mtas)_2]^{+} \quad (2)$$

$$[Co(mtas)_2]^{+} + e^- \rightleftharpoons [Co(mtas)_2]^{0} \quad (3)$$

(BPh$_4$)$_2$ in acetonitrile containing 0.1 M Bu$_4$NPF$_6$ shows the same three redox processes (two reductions, one oxidation) plus an irreversible multielectron oxidation of BPh$_4^-$ with an oxidation peak potential E_p^{ox} = 0.83 V vs SCE (scan rate = 100 mV s^{-1}). As demonstrated by the data in Table 1, half-wave potentials ($E_{1/2}$ values) for each of the three redox processes do not depend on the initial oxidation state of the complex or the anion of the complex or chosen noncomplexing electrolyte. In dichloromethane-(0.1 M Bu$_4$NPF$_6$), [Co(mtas)$_2$](BPh$_4$)$_2$ exhibits chemically reversible [Co(mtas)$_2$]$^{3+/2+}$ and [Co(mtas)^2]$^{2+/+}$ couples but further reduction gives rise to a multielectron irreversible process. The potential difference ($\Delta E_{1/2}$) between the [Co(mtas)$_2$]$^{3+/2+}$ and [Co(mtas)$_2$]$^{2+/+}$ couples is slightly larger in dichloromethane (0.71 V) than in acetonitrile (0.65 V). The larger ΔE_p values in dichloromethane are attributed to uncompensated solution resistance.

To further characterize the redox chemistry (eqs 1−3), a spectroelectrochemical investigation of [Co(mtas)$_2$](BF$_4$)$_3$ was carried out in acetonitrile(0.1 M Bu$_4$NPF$_6$) at −20 °C. Conversion from one oxidation state to the next occurs efficiently (see Figure 2) with no complications such as adsorption or irreversible homogeneous reactions. The mtas ligand is nonabsorbing apart from the aromatic $\pi-\pi^*$ absorption band above 40 000 cm^{-1}, which facilitates interpretation of the ultraviolet and visible spectra. Cobalt-59 NMR studies have demonstrated octahedral CoAs$_6$ coordination for [Co(mtas)$_2$](BF$_4$)$_3$,[9] and the optical spectrum of [Co(mtas)$_2$]$^{3+}$ is dominated by an intense ligand to metal charge transfer (LMCT) band (As(σ) → Co("e_g")) centered near 36 000 cm^{-1} (Figure 2a). This is consistent with attributing an optical electronegativity of approximately 2.75 to mtas and a 10Dq value of approximately 25 000 cm^{-1} to the Co(III) complex.[14] Reduction to low-spin d^7 [Co(mtas)$_2$]$^{2+}$ displaces the charge transfer transition to only slightly

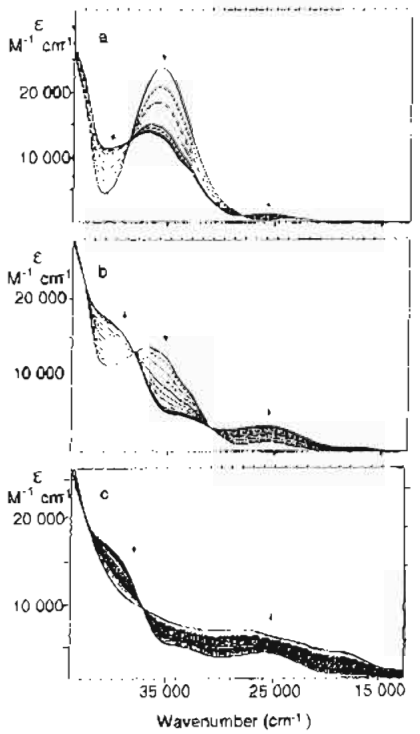

Figure 2. Spectroelectrochemical monitoring in acetonitrile containing 0.1 M Bu$_4$NPF$_6$ at −20 °C of the oxidation of (a) [Co(mtas)$_2$]$^{2+}$ to [Co(mtas)$_2$]$^{3+}$, (b) [Co(mtas)$_2$]$^+$ to [Co(mtas)$_2$]$^{2+}$, and (c) [Co(mtas)$_2$] to [Co(mtas)$_2$]$^+$.

higher energy, through the opposed contributions of decreased electronegativity and decreased 10Dq (10Dq ≈ 14 000 cm^{-1}, see below) in the five- or six-coordinate Co(II) ion. The LMCT band is further blue-shifted to nearly 40 000 cm^{-1} upon reduction to the d^8 Co(I) complex, which is very probably square-pyramidally or square-planar coordinated.[15] Weaker absorptions in the near-ultraviolet and visible spectra can be attributed to ligand field transitions in all three cationic complexes and these are described in detail in the following section. For [Co(mtas)$_2$]^0, the broad ultraviolet−visible envelope is typical of the presence of a ligand-centered radical,[16] indicating reduction of mtas on the Co(I) center. Thus, the spectra of Figure 2 are consistent with the stepwise formation of Co(II) and Co(I) species with the third reduction being ligand centered. It is important for the purposes of the present study to note that [Co^I(mtas)$_2$]$^+$ has appreciable stability. Furthermore, even [Co(mtas)$_2$]^0 is fully stable (for hours) and efficiently recycled in the spectrometer to its Co(I,II,III) precursors under the conditions described.

Solid and Solution Phase Ligand Field Spectra of [Co(mtas)$_2$](BF$_4$)$_3$ and [Co(mtas)$_2$](BPh$_4$)$_2$. In order to investigate the structural and electronic correspondence between species involved in solution and solid phase voltammetry for the Co(III)/Co(II) couple, electronic spectra of [Co^{III}(mtas)$_2$](BF$_4$)$_3$ and [Co^{II}(mtas)$_2$](BPh$_4$)$_2$ were measured in solution (acetonitrile) and in the solid state by diffuse reflectance. The spectra shown in Figure 3, focus on the visible/near-ultraviolet region only, because this region is expected to be most sensitive to the coordination geometry of the metal ion. Furthermore, absorption peaks in the ultraviolet region are severely flattened in the reflectance mode, making meaningful comparisons with solution spectra difficult. Figure 3 shows clearly that for each complex,

(14) Lever, A. B. P. *Inorganic Electronic Spectroscopy*, 2nd ed.; Elsevier: Amsterdam, 1984; pp 218−225.
(15) Cotton, F. A., Wilkinson, G. *Advanced Inorganic Chemistry: a Comprehensive Text*, 5th ed.; Wiley: New York, 1988; p 725.
(16) Heath, G. A., Lesley, J. H. *J. Chem. Soc., Dalton Trans.* **1983**, 1587.

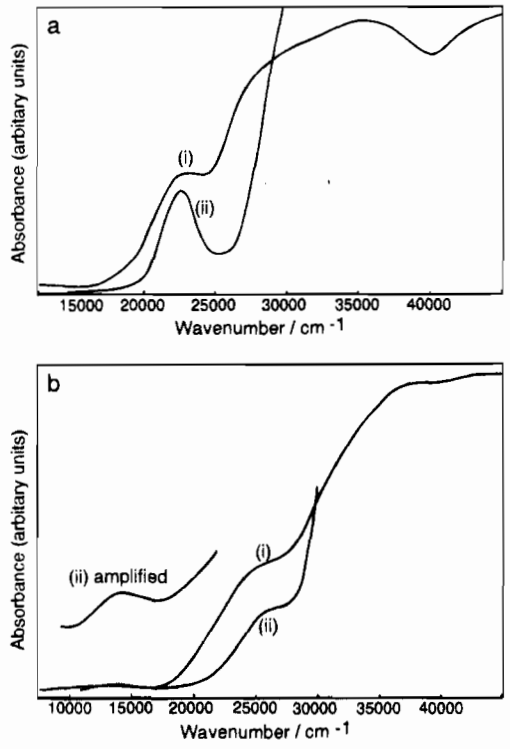

Figure 3. Solid state diffuse reflectance spectra (i) and solution (acetonitrile) spectra (ii) of (a) $[Co(mtas)_2](BF_4)_3$ and (b) $[Co(mtas)_2](BPh_4)_2$.

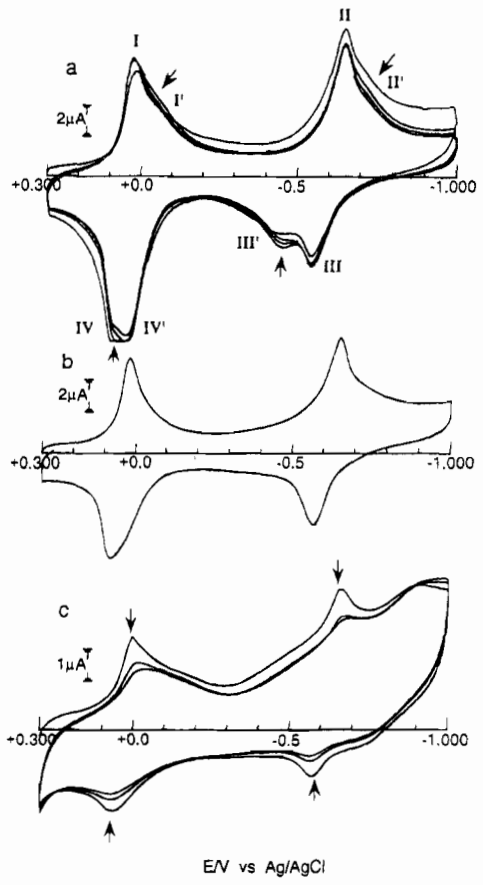

Figure 4. Cyclic voltammograms obtained in aqueous (0.1 M $LiClO_4$) electrolyte for solid $[Co(mtas)_2](ClO_4)_3$ mechanically attached to a basal plane pyrolytic graphite electrode (scan rate = 100 mV s^{-1}): (a) first four cycles; (b) eleventh cycle ("steady-state" response); (c) first three cycles after addition of 10 μM $NaBPh_4$.

the solution and solid phase samples exhibit the same spectroscopic features. This strongly suggests that the *structural and electronic changes in the primary coordination sphere that accompany the* Co(III)/Co(II) *redox reaction are the same in solid and solution.*

The ligand field spectra show features in common with Co(III) and Co(II) complexes with similar coordination spheres. Thus, for octahedral $[Co(mtas)_2](BF_4)_3$ (Figure 3a) the first spin-allowed d−d band is seen at 23 000 cm^{-1}, appropriately blue-shifted from the corresponding band near 17 000 cm^{-1} in $[Co(mtas)Br_3]$.[10] This band is derived from octahedral $^1A \rightarrow {}^1T_1$ and the accompanying $^1A \rightarrow {}^1T_2$ transition is expected[17] between 28 000 and 30 000 cm^{-1}, but where it would be concealed by the edge of the intense LMCT band. Faint shoulders at 17 000 and 13 000 cm^{-1} in the Co(III) reflectance spectrum may represent spin-forbidden transitions to $^3T_1$ and $^3T_2$, or (at 17 000 cm^{-1}) a low-symmetry component of $^1T_1$.

For $[Co(mtas)_2](BPh_4)_2$ (Figure 3b), there is a weak but distinct band near 14 000 cm^{-1} and a stronger one near 26 000 cm^{-1}. Throughout this region, the optical spectrum is reminiscent of low-spin $[Co(diars)_3]^{2+}$ (diars = 1,2-bis(dimethylarsino)benzene) but also of low-spin square-pyramidal $[Co(diars)_2X]^+$ sharing the $...(z^2)^1(x^2 - y^2)^0$ ground-state.[18] The electronic spectra of such Jahn−Teller elongated or five-coordinate low-spin Co(II) complexes are notoriously varied in detail,[19] and it is stressed that a distinction between five- and six-coordination cannot be made on the basis of these spectra. However, we regard the 14 000 cm^{-1} band as good indication of the effective 10*Dq* (corresponding to in-plane $xy \rightarrow x^2 - y^2$, and/or nearly iso-energetic $xz, yz \rightarrow z^2$). The higher energy band has variously been attributed to the $xz, yz \rightarrow x^2 - y^2$ transition or to low intensity $As(\sigma) \rightarrow x^2 - y^2$ charge transfer, possibly the spin-forbidden analog of the intense LMCT transition near 35 000 cm^{-1}. For the present purpose, the important point is that we have a sensitive two-band fit between the Co(II) microcrystalline solid and solution spectra, which implies that a common structure exists in the solid and solution phases.

Voltammetry of Microcrystalline $[Co(mtas)_2](ClO_4)_3$ and $[Co(mtas)_2](ClO_4)_2$. Figure 4a shows cyclic voltammograms of the initial and subsequent three cycles (scan rate = 100 mV s^{-1}) for microcrystalline $[Co(mtas)_2](ClO_4)_3$ mechanically attached to a basal plane pyrolytic graphite electrode in aqueous medium containing 0.1 M $LiClO_4$ as the electrolyte. Two well-defined reduction processes are seen within the aqueous electrolyte limit with each redox process exhibiting evidence of chemical reversibility. Complexity is noted in the form of peak splitting giving rise to peaks designated I, I′, II, II′, III, III′, IV, and IV′ as assigned in Figure 4a. On repeat scans the reduction components at more negative potentials (I′ and II′) become relatively less important than I and II and for the oxidation processes, features III′ and IV′ diminish. That is, the dominant persistent peaks are I, IV, II, and III. The cyclic voltammogram obtained after a further 10 scans over the potential range +0.3 to −1.0 V is given in Figure 4b. This and subsequent scans become essentially independent of the number of scans and in this sense represent a "steady state" dominated by peaks I, II, III, and IV. There is significant variation in peak currents but not in peak potentials for independent electrode preparations (attachments of solid), and indistinguishable electrochemistry is observed when 0.1 M

(17) Reference 14, pp 473−478 and Table 6.16.
(18) Dyer, G.; Meek, D. W. *J. Am. Chem. Soc.* **1967**, *89*, 3983.
(19) Reference 14, pp 490−493 and Table 6.20.

$KClO_4$ replaces 0.1M $LiClO_4$ as the electrolyte. Voltammetric data obtained from the typical "steady-state" response are given in Table 1.

The two redox processes observed for the solids clearly correspond to the first two reduction steps observed in nonaqueous solvents, and should result in the formation of Co(II) and Co(I) species. In support of this assumption, $\Delta E_{1/2}$ values are noted to be very similar for the dissolved complex in acetonitrile and dichloromethane (0.65 and 0.71 V, respectively) and for the microcrystalline solid in aqueous solution (0.66 V). Even the absolute values of the potentials are remarkably convergent. The correlation in optical spectra of microcrystalline and solution phases for each oxidation state described above are the best evidence to hand that the solution phase redox transformations are faithfully reflected in the solid phase. However, the shape and scan rate dependence of the responses is markedly different for the solid and dissolved complex. In organic solvents where the complexes are soluble, the expected diffusion controlled shape is obtained at all scan rates examined (50−500 mV s^{-1}). In contrast, voltammetry of the solid gives much sharper peaks and, for the Co(III)/Co(II) couple, ΔE_p values are very small at slow scan rates. (For example, for the electrode preparation corresponding to the data in Table 1, ΔE_p = 42 mV at 5 mV s^{-1}.) Additionally, there is an approximately linear relationship between peak current (i_p) and scan rate (v) (rather than with $v^{1/2}$) over the range 5−500 mV s^{-1} for both processes.

The main features of the voltammetric response of the microcrystalline cobalt solid are not consistent with diffusion control. Rather, they have the characteristics of thin layer electrochemistry.[20] This may originate from complete electrolysis of particles which are sufficiently small that diffusion is not relevant and/or from the presence of thin layers of electroactive material on the outer surface of relatively large particles. From the known electrode area, and observed current, we can draw some tentative conclusions concerning the physical nature of the electrode state. For two independent electrode preparations, integration of the current under peaks I and III in the cyclic voltammograms gave charges which would equate to surface coverages of electroactive material of 3.3×10^{-10} and 6.4×10^{-10} mol cm^{-2} (reduction of $[Co(mtas)_2]^{3+}$) and 2.7×10^{-10} and 5.4×10^{-10} mol cm^{-2} (oxidation of $[Co(mtas)_2]^{+}$). In the following calculation, we therefore adopt an indicative surface coverage value of 4×10^{-10} mol cm^{-2}. Electron microscopy reveals that approximately 1% of the electrode surface is covered with solid. For cube-shaped particles with five faces exposed, the total solid/electrolyte interface is then approximately 5% of the electrode surface area. If the reasonable assumption is made that monolayer coverage corresponds to 1×10^{-10} mol cm^{-2},[3,4] it is apparent that the proposed electroactive layers on the surfaces of microcrystals have a thickness of the order of 100 stacked redox-active monolayers. For the observed average particle diameter of 10 μm, this represents a small fraction of the total solid (i.e. a thin layer). The similarity of voltammetric response in $LiClO_4$ and $KClO_4$ electrolytes is expected for thin layer processes which are not limited by diffusion processes. Clearly, under these conditions, it is impossible via voltammetric measurements alone to gain information concerning the uptake and expulsion of counterions associated with electron transfer.

Several explanations may be proposed for the secondary processes observed (features I′, II′, III′ and IV′ in Figure 4a): for example, a minor component of thick-layer (i.e. diffusion controlled) behavior arising from the oxidation of the bulk of larger particles or alternatively the presence of different phases in the oxidized or reduced forms of the solid. The broadness of responses I′, II′, and III′ and other features point to the former explanation which, as discussed below, accounts for the experimental data in a qualitative manner.

(20) Reference 13, pp 409−413.

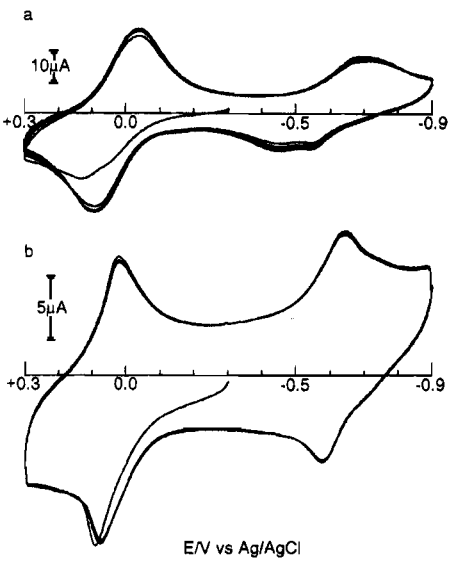

Figure 5. Cyclic voltammograms obtained in aqueous (0.1 M $LiClO_4$) electrolyte for solid $[Co(mtas)_2](ClO_4)_2$ mechanically attached to a basal plane pyrolytic graphite electrode (scan rate = 100 mV s^{-1}): (a) first six cycles; (b) cycle after forty repeat cycles.

The influence of the anion of the supporting electrolyte on the electrochemical response could not be systematically studied because of the solubility of the solid in most electrolytes other than perchlorates. However, the effect of $NaBPh_4$ was examined briefly. At a concentration of 0.1 M, the current from the oxidation of BPh_4^- obscures the response of the cobalt complex and hence only a small amount (approximately 10 μM) of $NaBPh_4$ was added to the 0.1 M $LiClO_4$ electrolyte. As shown in Figure 4c, this leads to a significant decrease in all peak currents, and a new couple appears at approximately −0.82 V. (This couple is not due to reduction of an oxidation product of BPh_4^-). Evidently, BPh_4^- blocks the transfer of ClO_4^- across the solid/solution boundary; the same effect was observed for microcrystalline decamethylferrocene on addition of small amounts of $NaBPh_4$ to the perchlorate electrolyte.[5] The same studies also demonstrated that redox processes accompanied by uptake and expulsion of BPh_4^- are thermodynamically more difficult (occurring at more positive potentials for oxidation of decamethylferrocene) than those involving ClO_4^-. Hence it is reasonable to assign the new couple at −0.82 V to the Co(III)/Co(II) or (more probably) Co(II)/Co(I) redox reaction with transport of BPh_4^- coupled to electron transfer. Changes in response are obvious in the first cycle after addition of BPh_4^- (compare Figure 4b and the first scan of Figure 4c) and hence it appears that exchange of ClO_4^- for BPh_4^- occurs, to some extent, at an open circuit (i.e. prior to the first scan in the presence of BPh_4^-).

The voltammetry of divalent microcrystalline $[Co(mtas)_2](ClO_4)_2$ was also investigated in aqueous (0.1 M $LiClO_4$) medium. The electrode response of the mechanically attached Co(II) salt is noticeably distinct from the Co(III) salt on initial scans (Figure 5a) but converges on repeated cycling. For the Co(II) form of the complex, the contribution of the diffusion controlled current is considerably larger and the response requires considerably more cycling of the potential to reach the "steady state". After 40 repeat scans over the potential range

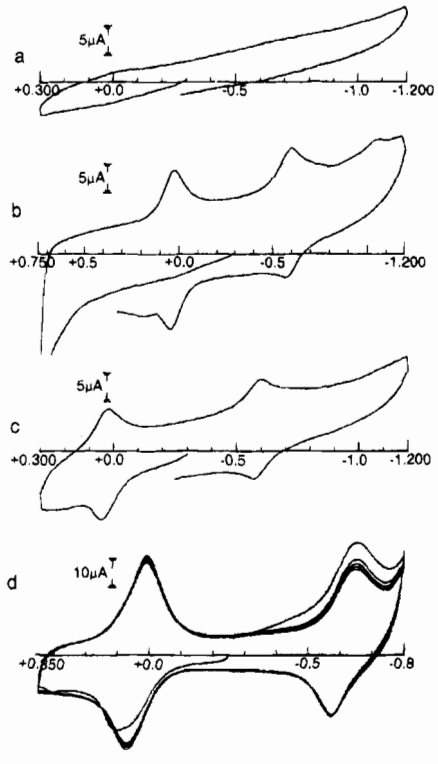

Figure 6. Cyclic voltammograms obtained in aqueous (0.1 M $LiClO_4$) electrolyte (curves a–c) for solid $[Co(mtas)_2](BPh_4)_2$ mechanically attached to a basal plane pyrolytic graphite electrode (scan rate = 100 mV s^{-1} (a–c); 500 mV s^{-1} (d)). (a) first cycle over the potential range −1.2 to +0.3 V; (b) first cycle after holding the potential at 0.75 V for 120 s; (c) cycle 11 over the potential range −1.2 to +0.3 V; (d) separate electrode preparation, 0.1 M $KClO_4$ electrolyte, cycles 11–15 after holding the potential at 0.75 for 120 s.

+0.3 to −0.9 V, the response (Figure 5b and Table 1) is similar to that for $[Co(mtas)_2](ClO_4)_3$ (Figure 4b).

Voltammetry of Microcrystalline Solid $[Co(mtas)_2](BPh_4)_2$ and X-ray Electron Probe Analysis. In order to investigate the role of the anion in the solid, the voltammetry of solid $[Co(mtas)_2](BPh_4)_2$ mechanically attached to a graphite electrode was examined. Figure 6a shows the response when the electrode is placed in aqueous (0.1 M $LiClO_4$) electrolyte and the potential is cycled over the region +0.3 to −1.2 V. Only very low currents are observed at the potentials expected for the Co(III)/Co(II) and Co(II)/Co(I) couples when $[Co(mtas)_2](BPh_4)_2$ is attached to the electrode. This is an important observation in a general sense because it illustrates that the voltammetric response of a given complex ion in the form of its mechanically attached microcrystalline salt can vary from nil to well-defined and informative, depending on the counterion. However, extending the potential range to 0.75 V and holding the potential for 120 s leads to dramatically larger currents for both redox processes (Figure 6b), and a new reduction process also appears at $E_p^{red} = -1.0$ V (scan rate = 100 mV s^{-1}). Holding the potential at 0.3 V where oxidation of $[Co(mtas)_2]^{2+}$ occurs does not have the same effect. Oxidation of BPh_4^- occurs at 0.75 V and, by analogy with the oxidation of BH_4^-, is assumed to involve a complex mechanism ultimately giving BO_2^- or some intermediate redox product.[21] Evidently, conversion of BPh_4^- to a smaller and more hydrophilic anion, is necessary before electron transfer with accompanying ion movements can take place at an appreciable rate. The potentials for the Co(III)/Co(II) and Co(II)/Co(I) couples (Table 1) are the same as those

(21) Reference 1, Vol. II (1974), Chapter 1.

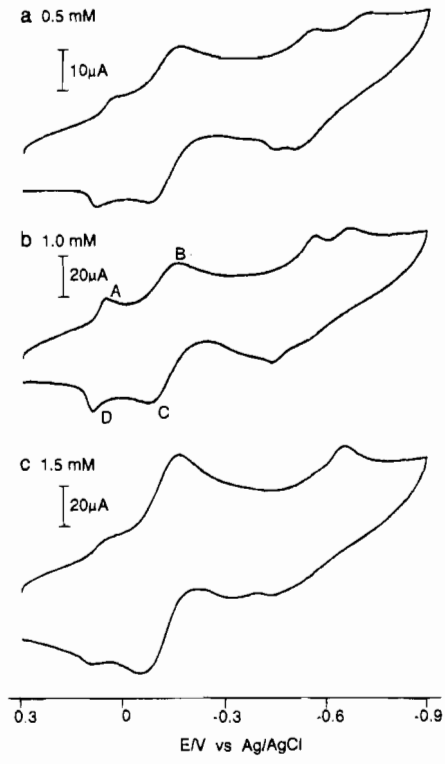

Figure 7. Cyclic voltammograms obtained in aqueous (0.1 M LiCl) electrolyte at a basal plane pyrolytic graphite electrode (scan rate = 100 mV s^{-1}) for dissolved $[Co(mtas)_2](BF_4)_3$ at the following concentrations: (a) 0.5 mM; (b) 1.0 mM; (c) 1.5 mM.

for $[Co(mtas)_2](ClO_4)_3$ and $[Co(mtas)_2](ClO_4)_2$ suggesting that exchange of BO_2^- or another anion for ClO_4^- takes place during oxidation at 0.75 V. The new redox process at a more negative potential may arise from reduction of Co(III) or Co(II) coupled to BPh_4^- transport. After the potential was cycled a further 10 times over the range +0.3 to −1.2 V, the scan shown in Figure 6c was recorded. Disappearance of the reduction peak at −1.0 V is consistent with exchange of mobile BPh_4^- for ClO_4^- during repeat redox cycling. The voltammetry in 0.1 M $KClO_4$ is indistinguishable to that found with 0.1 M $LiClO_4$ implying that the nature of the cation is unimportant although in both electrolytes there is significant variation in peak currents and ΔE_p values for separate electrode preparations. For example at 500 mV s^{-1}, the reduction peak current for the Co(III)/Co(II) couple varies from 4.6 to 45 μA for ten electrode preparations and ΔE_p ranges from 43 to 77 mV; larger ΔE_p values are associated with larger peak currents. The response (recorded at a scan rate 500 mV s^{-1} in 0.1 M $KClO_4$) for a separate electrode preparation is given in Figure 6d for comparison. There is always an approximately linear dependence between peak currents and scan rate for the Co(III)/Co(II) couple and ΔE_p values are generally smaller than expected for a diffusion controlled process. For the Co(II)/Co(I) couple, the peak current dependency on scan rate, v, is between $v^{1.0}$ and $v^{1/2}$, and the reduction peak is broad at slow scan rates, which is consistent with a mixture of thin and thick layer behavior, with thick layer behavior dominant at slower scan rates.

The redox reactions and charge transport processes in the BPh_4^- salt were further investigated by experiments involving electrolyses followed by analysis using X-ray electron probe microanalysis. Prior to analysis, the potential of the graphite electrode with the attached solid was held at 0.75 V for 120 s in 0.1 M $KClO_4$ and different potential programs were then applied to different samples: −0.8 V (120 s), −0.3 V (120 s);

−0.3 V(120 s), 0.3 V (120 s); −0.3 V (120 s), 0.3 V (120 s), −0.8 V (120 s). The electrode was then removed from solution, washed and returned to solution, and electrolyzed at 0.3 V (120 s). All particles on the surface ranging in size from 0.5 to 30 μm, analyzed after the various electrolysis programs described above, gave strong signals for Co and As but no signals due to Cl or K were detected for any sample. (Cl and K, if present, are readily detectable by electron probe analysis but sensitivity is very poor for lighter elements such as C, H, O, and B.) Small particles (≤0.5 μm in size) were discernible on the graphite surface but useful analyses of such particles could not be made because of the comparatively large analyzer window. Again these observations are consistent with the dominance of thin layer voltammetry in the particulate solid. X-ray electron probe analysis penetrates the bulk of the particles, and hence the presence of ClO_4^- or K^+ in an outer layer may give an immeasurably small signal. Alternatively redox chemistry and hence the uptake of electrolyte ions may only occur in small particles which cannot be satisfactorily analyzed.

In summary, the voltammetry of solid microcrystals of $[Co(mtas)_2](ClO_4)_n$ ($n = 2, 3$) may be summarized by eqs 4 and 5 and for $[Co(mtas)_2](BPh_4)_2$ the initial oxidation at 0.75 V is represented by eq 6 (where $x = 0-2$). Following oxidation of

$$[Co(mtas)_2](ClO_4)_3(solid) + e^- \rightleftharpoons [Co(mtas)_2](ClO_4)_2(solid) + ClO_4^-(soln) \quad (4)$$

$$[Co(mtas)_2](ClO_4)_2(solid) + e^- \rightleftharpoons [Co(mtas)_2](ClO_4)(solid) + ClO_4^-(soln) \quad (5)$$

$$[Co(mtas)_2](BPh_4)_2(solid) + (3-x)ClO_4^-(soln) + 4H_2O \rightarrow [Co(mtas)_2](ClO_4)_{3-x}(BO_2)_x(solid) + (2-x)BO_2^-(soln) + 8H^+ + 9e^- + \text{organic products} \quad (6)$$

$[Co(mtas)_2](BPh_4)_2$ reduction of the solid must take place by similar steps to those shown in eqs 4 and 5, although expulsion of BO_2^- may be involved.

Voltammetry of $[Co(mtas)_2](BF_4)_3$ Dissolved in Aqueous Media. The tervalent complex $[Co(mtas)_2](BF_4)_3$ is freely soluble in 0.1 M LiCl electrolyte, in contrast to the situation in 0.1 M $LiClO_4$ where the compound has low solubility. Parts a−c of Figure 7 show cyclic voltammograms recorded at a scan rate of 100 mV s^{-1} at a basal plane pyrolytic graphite electrode when 0.5, 1.0, and 1.5 mM solutions of $[Co(mtas)_2](BF_4)_3$ are prepared in aqueous 0.1 M LiCl. Significantly, the results are very concentration dependent, implying the presence of both surface and bulk solution processes. The first two processes can be assumed to correspond to the reduction of $[Co(mtas)_2]^{3+}$ to form $[Co(mtas)_2]^{2+}$ and the remaining processes then lead to formation of $[Co(mtas)_2]^+$. For the Co(III)/Co(II) couple, the response is suggestive of strong adsorption of $[Co(mtas)_2]^{2+}$ giving rise to an adsorption prepeak (A, Figure 7b) preceding the diffusion-controlled reduction (B) and an adsorption post-peak (D) following the diffusion-controlled oxidation (C).[22] Consistent with this interpretation, there is a linear dependence of i_p with v for peak D and i_p with $v^{1/2}$ for peak B over the scan rate range 20−200 mV s^{-1}. Thus peaks A and D can respectively be assigned to the forward and reverse reactions in eq 7 and peaks B and C to the solution phase couple. The

$$[Co(mtas)_2]^{3+}(soln) + e^- \rightleftharpoons [Co(mtas)_2]^{2+}(ad) \quad (7)$$

charge associated with peak A corresponds to a surface coverage of electroactive material of 3.7×10^{-10} mol cm^{-2} which is

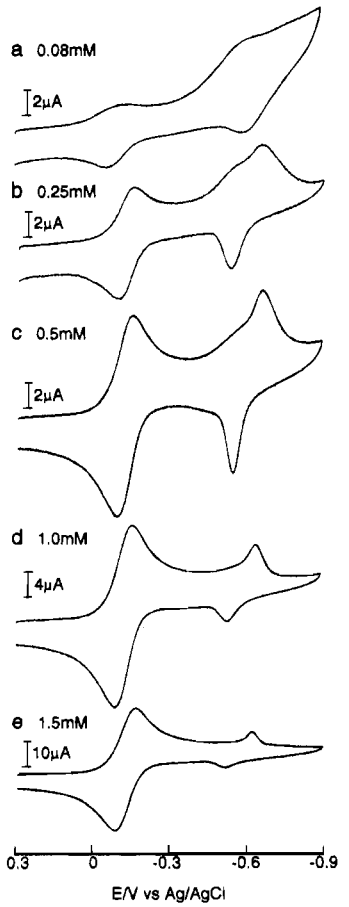

Figure 8. Cyclic voltammograms obtained in aqueous (0.1 M LiCl) electrolyte at a glassy carbon electrode (scan rate = 100 mV s^{-1}) for dissolved $[Co(mtas)_2](BF_4)_3$ at the following concentrations: (a) 0.08 mM; (b) 0.25 mM; (c) 0.5 mM; (d) 1.0 mM; (e) 1.5 mM.

greater than might be expected for monolayer coverage.[3,4] However, there is no evidence that access of solution-phase species to the surface is blocked by this deposit, implying that the deposit is porous or restricted to isolated areas on the electrode surface. The response for the Co(II)/Co(I) couple is more complex with two reduction and three oxidation components able to be discerned and the assignment of peaks to particular solution- or adsorption-based processes cannot be made with confidence. It is apparent (particularly for the 1.5 mM solution, Figure 7c) that the total current associated with the Co(II)/(I) couple is less than that for the Co(III)/Co(II) couple suggesting blocking of the electrode surface by adsorbed material.

The response at a glassy carbon electrode (Figure 8) is markedly different from that at basal plane pyrolytic graphite, as may be expected when surface-based processes are present. As shown for 0.08, 0.25, 0.5, 1.0, and 1.5 mM solutions of complex, there is no separate prepeak with the diffusion-controlled Co(III)/Co(II) couple but the anodic peak current is greater than the cathodic, which is again consistent with weak adsorption of $[Co(mtas)_2]^{2+}$.[22] This was confirmed by double potential-step chronocoulometry.[23] When the potential was stepped between +0.3 and −0.3 V for a 0.5 mM solution of complex, a plot of charge *vs* $t^{1/2}$ gave a surface excess of adsorbed $[Co(mtas)_2]^{2+}$ of 5×10^{-11} mol cm^{-2} (step time = 50 ms) and 1×10^{-10} mol cm^{-2} (step time = 100 ms).

At the lowest concentration of $[Co(mtas)_2](BF_4)_3$ (Figure 8a), the second redox step has the characteristics of a predominantly

(22) Reference 13, pp 519−532.
(23) Reference 13, pp 201−204.

diffusion-controlled process which is complicated by weak adsorption of both reactant and product. However, as the bulk concentration increases, sharp peaks indicative of strongly adsorbed material develop and the diffusion-controlled current associated with the Co(II)/Co(I) couple diminishes. For both 1 mM and 1.5 mM solutions, integration of the cathodic peak at $E_p^{red} \approx -0.66$ V (Figure 8d,e) gives 2×10^{-10} mol cm^{-2} of adsorbed electroactive material. Thus it appears that a self-limiting film of insulating $[Co(mtas)_2]Cl$ or $[Co(mtas)_2](BF_4)$ deposits on the glassy carbon electrode and completely blocks the further reduction of solution species.

Discussion

Three aspects of the present study offer new insights into the electrochemistry of nonconducting microcrystalline solids. First, the complexes $[Co(mtas)_2](ClO_4)_3$ and $[Co(mtas)_2](ClO_4)_2$ demonstrate typical thin layer electrochemistry with the electrolysis of only a small fraction of the total amount of solid coexisting giving small ΔE_p values. This type of electrochemistry has not been previously observed (as the dominant response) with microcrystalline solids. The different behavior of these solids relative to decamethylferrocene and *cis*- and *trans*-$Cr(CO)_2(dpe)_2$ and *trans*-$[Cr(CO)_2(dpe)_2]^+$ could originate from the higher charge of the electroactive species and the effect of this on ion-pairing energies in the solid. For redox and conducting polymers, ion-pairing has been demonstrated to contribute to both increased resistance to counterion migration and/or diffusion and decreased electron hopping rates.[24-26] The latter phenomenon has been treated theoretically.[27] In the case of microcrystalline solids, charge transfer is envisaged to start at the three-phase electrode/solid/solution boundary and then extend over the surface of the solid. For $[Co(mtas)_2](ClO_4)_3$ and $[Co(mtas)_2](ClO_4)_2$ complexes, it is proposed that *only at a thin hydrated outer layer* does disruption of ion-pairing allow a rapid rate of electron and ion transfer. In the bulk of the solid, the movement of counterions and electron-hopping rate is very low, leading to very low diffusion-controlled currents.

For all the mechanically attached solids, peak currents for the Co(II)/Co(I) step are lower than for the Co(III)/Co(II) couple and there is a larger contribution to the response from secondary (diffusion-controlled) processes. This observation may be accounted for by considering changes in hydrophobicity of the solid during redox cycling. As the surface layer is reduced it becomes more hydrophobic and hence the hydrated layer may thin resulting in fewer electroactive sites. However, at the same time, as some reduction of the bulk solid occurs, the strength of ion-pairing decreases and the diffusion-controlled contribution can become more important. The differences in the initial responses of $[Co(mtas)_2](ClO_4)_3$ and $[Co(mtas)_2](ClO_4)_2$ (Figures 4a and 5a) are consistent with this description. Clearly the contribution of diffusion-controlled components are relatively more important for $[Co(mtas)_2](ClO_4)_2$, and the strength of ion-pairing should be lower in this solid. On the other hand, $[Co(mtas)_2](ClO_4)_2$ is also the more hydrophobic solid and hence the greater number of potential cycles for hydration of the outer layer to reach the "steady state". The above model explains some aspects of the electrochemistry. However, it is not understood why on repeat scans (Figures 4a,b and 5a,b) the diffusion-controlled current decreases relative to the thin layer component.

The second interesting feature of the present study is the effect of BPh_4^- and its oxidation on the voltammetry of the solid. Tetraphenylborate is both a very hydrophobic and very bulky anion (in comparison with ClO_4^-), but the former property appears to be most important in this context. Thus, the depression of peak currents for the reduction of $[Co(mtas)_2](ClO_4)_3$ when a small amount of $NaBPh_4$ is added to the electrolyte is consistent with partitioning of BPh_4^- from aqueous solution into the more hydrophobic solid phase, and exchange with ClO_4^- and/or blocking of its transport. For microcrystalline $[Co(mtas)_2](BPh_4)_2$, the hydrophobicity of BPh_4^- is proposed to prevent surface hydration, but the possible oxidative conversion to a more hydrophilic anion and uptake of ClO_4^- facilitates surface hydration.

Finally of importance in this study is the availability of a comparison of voltammetry in aqueous media of dissolved and solid phases. The comparison reveals two interesting aspects of the electrochemistry of solids. The first concerns the thermodynamics of redox processes in the mechanically attached solids. The potential of the solid phase Co(III)/Co(II) couple is approximately 170 mV more positive than that for the aqueous solution species whereas the Co(II)/Co(I) couple appears near the same potential in both phases. At least three factors must be considered when attempting to account for the redox potentials observed in microcrystalline solids, in comparison to those obtained for aqueous solution species: first, the relative free energies of transport of an electrolyte anion across the solution/solid interface for both oxidation states of solid involved in the redox couple, second, differences in molecular structure between solid and solution species, and finally, the relative stabilization of each species of the redox couple in the solid environment. For the system under study, the first term may be assumed to be relatively unimportant because, under conditions of predominantly thin layer voltammetry, there is likely to be negligible dependence on (and hence a negligible free energy term arising from) ion transport. It also seems unlikely that structural differences between the solution and the solid species lead to the difference in Co(III)/Co(II) potentials. Comparisons of solution and solid phase spectra for each oxidation state reveal that when prepared as the bulk materials, the molecular structures in the solid are indistinguishable from those in solution. While this does not necessarily mean that the same is true on the short time scale of cyclic voltammetric experiments, any structural differences are more likely to be associated with the Co(II) or Co(I) complexes than the tervalent species and hence to be manifested in potential shifts for the Co(II)/Co(I) couple. Evidently, this is not observed. On the other hand, it is reasonable to propose that the stabilization of $[Co(mtas)_2]^{3+}$ relative to $[Co(mtas)_2]^{2+}$ in aqueous solution is significantly greater than in the solid, due to the effects of hydration and ion−dipole interactions in the solution phase. Such stabilization effects are known to decrease with ion charge and hence the similarity of potentials for the Co(II)/Co(I) couples (Table 1) in both phases. Supporting this proposal are the results of voltammetry in organic solvents where the potential for the Co(III)/Co(II), but not the Co(II)/Co(I), couple depends on the solvent (acetonitrile or dichloromethane). However, given the complexity of the redox process in the mechanically attached solid, it is nevertheless surprising that the potential of the Co(II)/Co(I) couple is the same in both solid and solution phases and this might result from the cancellation of opposing effects.

The second interesting aspect of the voltammetry of $[Co(mtas)_2](BF_4)_3$ dissolved in aqueous medium relates to the formation of electrodeposits. Comparisons between results obtained at glassy carbon and basal plane graphite electrodes enable the importance of the morphology of surface-confined solid to be probed. Thus, at glassy carbon, relatively small

(24) Ren, X.; Pickup, P. G. *J. Phys. Chem.* **1993**, *97*, 5356.
(25) Oh, S. M.; Faulkner, L. R. *J. Electroanal. Chem.* **1989**, *269*.
(26) Ren, X.; Pickup, P. G. *J. Electroanal. Chem.* **1994**, *365*, 289.
(27) Saveant, J.-M. *J. Phys. Chem.* **1988**, *92*, 4526.

amounts of adsorbed material (2×10^{-10} mol cm^{-2} $[Co(mtas)_2]$-Cl or $[Co(mtas)_2](BF_4)$) block the electrode surface, presumably because the deposit forms a continuous, pinhole-free electrochemically insulating layer. However, under different conditions, larger amounts of surface-confined material (in the present study, up to 6.4×10^{-10} mol cm^{-2} for mechanically attached solids and 3.7×10^{-10} mol cm^{-2} for electrodeposited $[Co(mtas)_2](BF4)_{2-x}Cl_x$ ($x = 1-2$) on basal plane graphite) may be electroactive. For both these cases, it is assumed that the electrode deposit is microparticulate, and hence these results highlight the importance of the relatively large edge to total solid area ratio for the voltammetry of solids.

Conclusions

These studies illustrate that the observed electrode response of (mechanically attached) microcrystalline salts of a given complex cation can be decisively influenced by the identity of the counteranion. In the present context of insoluble $[Co(mtas)_2]^{2+,3+}$ salts immersed in aqueous electrolytes, this response ranges from a well defined and faithful reflection of the solution-phase couples (ClO_4^-) to virtual suppression of informative signals (as with BPh_4^-, prior to electroconditioning). The latter phenomenon is attributed to the relative hydrophobicity of the microcrystalline BPh_4^- salts. Potential data for the solid and dissolved species in aqueous media reveal that the thermodynamics of solid-based redox couples can be significantly different from those of analogous couples in solution but, perhaps more surprisingly, can also be very similar. Finally, the importance of microcrystallinity to the observation of well-defined electrochemistry is demonstrated by comparisons with electrodeposited films of the same material.

Acknowledgment. We thank Denise R. Fernando (School of Agriculture, La Trobe University) and Denes Bogsanyi (Research School of Chemistry, Australian National University) for technical assistance. The authors also gratefully acknowledge extensive discussions with Frank Marken and financial support from the Australian Research Council. A.J.D. thanks the University of Canterbury for the granting of study leave.

IC941340M